

Charge and spin addition energies of a one-dimensional quantum dot

T. Kleimann,¹ M. Sasseti,¹ B. Kramer,^{1,*} and A. Yacoby²

¹*Dipartimento di Fisica, INFN, Università di Genova, Via Dodecaneso 33, 16146 Genova, Italy*

²*Department of Condensed Matter Physics, The Weizmann Institute of Science, Rehovot, 76100 Israel*

(Received 7 March 2000; revised manuscript received 28 April 2000)

We derive the effective action for a one-dimensional electron island formed between a double barrier in a single-channel quantum wire including the electron spin. Current and energy addition terms corresponding to charge and spin are identified. The influence of the range and the strength of the electron interaction and other system parameters on the charge and spin addition energies and on the excitation spectra of the modes confined within the island is studied. We find by comparison with experiment that spin excitations in addition to nonzero range of the interaction and inhomogeneity effects are important for understanding the electron transport through one-dimensional quantum islands in cleaved-edge-overgrowth systems.

I. INTRODUCTION

Recently, considerable progress in the science and technology of semiconductor nanostructures has been made. The experimental realization of one-dimensional (1D) quantum wires has opened new routes to investigating the influences of interactions and impurities on electron transport at low temperatures where quantum effects dominate.¹⁻³ In spite of numerous theoretical results obtained for the Luttinger liquid model,⁴⁻⁶ which have been used for interpreting the data, complete physical understanding of the experiments has not been achieved yet. It is therefore useful to study microscopically the combined effects of interactions and impurities on 1D quantum transport within more realistic models and to compare the results with experimental data.

The Luttinger liquid model allows one to take into account interactions between fermions in one dimension exactly. The linear conductance of a clean, infinitely long (spin degenerate) Luttinger liquid has been predicted to be $G = 2e^2 g_\rho / h$, the universal conductance renormalized by an interaction constant g_ρ .⁷ However, dc transport experiments on quasi-1D semiconductor quantum wires at relatively high temperatures showed only quantization in terms of the universal conductance $G = 2e^2/h$. This has been interpreted either in terms of a compensating, self-consistent renormalization of the external electric driving field⁸⁻¹⁰ or the use of noninteracting leads connected to the quantum wire¹¹⁻¹³ that eventually determine the conductance. However, at lower temperatures, temperature-dependent deviations from the universal conductance steps have been found:

$$\delta G \propto T^\kappa \quad (1)$$

($\kappa < 0$). This has been attributed to weak scattering at the random impurity potential in a Luttinger liquid.¹⁴

When the electron density in the GaAs/Al_xGa_{1-x}As quantum wires fabricated by using the cleaved-edge-overgrowth technique is decreased by applying a voltage to an external gate, eventually even the lowest electronic subband can be depopulated¹⁵ and the region of Coulomb blockade reached. Here, the mean electron density is sufficiently low, such that only very few maxima of the random potential of the impu-

rities are higher than the Fermi level. A 1D quantum island can be formed between two potential maxima in such a wire. Electron transport is then dominated by charging effects.¹⁶⁻¹⁸ At temperatures lower than the charging energy, the linear conductance shows discrete peaks corresponding to transferring exactly one electron through the quantum island.

In this region, it has been detected that the temperature dependence of the intrinsic width Γ of several conductance peaks is modified by the correlations between the electrons and, instead of being independent of T , shows nonanalytical power-law behavior ($\lambda > 0$):

$$\Gamma(T) \propto T^\lambda. \quad (2)$$

Such a behavior has been predicted in the sequential tunneling regime for resonant transport through a quantum dot coupled to a spinless Luttinger liquid¹⁹ and for a double barrier in a Luttinger liquid.^{20,21}

In nonlinear transport, collective excited states of the electrons in the island can contribute.^{22,23} The low-temperature current-voltage characteristics shows fine structure within the ‘‘Coulomb steps,’’ which reflects the excitation spectrum of the electrons in the quantum dot. Especially in one dimension, strong effects of the spin of the correlated electrons have been predicted by using a sequential tunneling model combined with the exact spectrum of eigenvalues and the corresponding states.²⁴ In the above mentioned experiments,¹⁵ contributions of the excited states in the 1D island have been found. In addition, one of the corresponding peaks in the differential nonlinear conductance showed an interaction-induced nonanalytical temperature dependence consistent with the above Luttinger liquid behavior (2). Thus, correlations beyond the phenomenological charging model seem to be present in these semiconductor quantum wires. This is also indicated by recent results of Raman scattering experiments, which strongly suggest that semiconductor quantum wires are very probably dominated by non-Fermi liquid behavior.²⁵ In view of the existing broad theoretical understanding of 1D non-Fermi liquids,²⁶ it is highly desirable to provide quantitative results for charging and correlation phenomena in these systems by using reasonably realis-

tic and controllable models, including the nonzero range interaction between the electrons as well as the potential of the impurities.

Efforts in this direction have been made by studying transport through a single barrier in a Luttinger liquid including long-range interactions.^{27–30} Charging in the presence of two impurities has been studied for spinless electrons with an interaction range much smaller than the distance between the two impurities.³¹ The crossover from a Luttinger liquid with a long-range interaction to a Wigner crystal in the presence of two symmetrically arranged potential barriers has been investigated.³²

In the present paper, we establish the fundamentals of a transport theory for 1D quantum dots embedded in a 1D electron system of correlated electrons *with spin*, which turns out to be considerably different from the spinless case. Especially, we concentrate here on the energies for charge and spin additions to the electron island formed between two strong impurities in a single-channel quantum wire of diameter d with an electron interaction of nonzero range. The quantum wire is described by using the Luttinger liquid model with spin.²⁶ The bias electric field is assumed to have an arbitrary spatial shape. The interaction is assumed as a 3D Coulomb potential, which we project to one dimension by using the Gaussian wave function associated with the lowest state in a parabolic, cylindrically symmetric confinement potential. Screening is introduced by an infinite metallic plane at a distance D parallel to the wire. For comparison, we comment also on results obtained for a projected screened 3D Coulomb interaction.

With the imaginary-time path-integral method, we determine the effective action in which charging and transport contributions are identified. The strength and the range of the interaction, V_0 and D , respectively, and the length of the 1D quantum island—the distance between two δ -function-like potential barriers a —determine characteristic energy scales related to the charge and spin excitations that appear in the model. We find that the characteristic energy related to the addition of charge to the island—the *charging energy*—always increases with increasing interaction range until it saturates when the latter exceeds considerably the length of the island. On the other hand, the energy related to the addition of a spin—the *spin addition energy*—is approximately the same as that of noninteracting particles induced by the Pauli principle. This is due to the smallness of the (short-ranged) exchange interaction.

We observe that the spatial shape of the electric field enters the effective action. The corresponding term can be interpreted as simulating the influence of the voltage at a gate electrode in experimental realizations.

Using our results, we have analyzed recent experimental data.¹⁵ We attempted to deduce the parameters of the quantum wire used in the experiment quantitatively. We found that it is not possible to identify a region of parameters that is consistent with *all* of the experimental findings. We conclude that depending on the quantity considered, the frequency spectra of the collective excitations, or the temperature dependence of the peaks in the differential conductance, experiments probe the interaction in different regions of the 1D sample, namely, within the island itself or within the whole quantum wire extending along the edge of the sample. This

indicates that, together with spin and finite interaction range, inhomogeneity effects have to be taken into consideration for understanding the quantum transport in these 1D semiconductor systems.

The paper is organized as follows. Section II briefly describes the model. In Sec. III, the effective action is provided and discussed. In Sec. IV we comment on the conditions of current transport. Quantitative results for the charging energy are given in Sec. V. Finally, we analyze experimental data in Sec. VI.

II. THE MODEL

A. The Hamiltonian

We use the bosonization technique^{6,26} for interacting electrons with spin in one dimension. The quantum dot is described by a double barrier consisting of two δ -function potentials $V_i\delta(x-x_i)$ at x_i ($i=1,2$) where $x_1 < x_2$. An external electric field $\mathcal{E}(x,t) = -\partial_x U(x,t)$ is assumed to induce transport. The Hamiltonian is

$$H = H_0 + H_B + H_U. \quad (3)$$

The first term describes the interacting electrons within the Luttinger liquid model,^{4,5}

$$\begin{aligned} H_0 = & \frac{\hbar v_F}{2} \int dx \{ \Pi_\rho^2(x) + [\partial_x \vartheta_\rho(x)]^2 \} \\ & + \frac{1}{\pi} \int dx \int dx' \partial_x \vartheta_\rho(x) V(x-x') \partial_{x'} \vartheta_\rho(x') \\ & + \frac{\hbar v_\sigma g_\sigma}{2} \int dx \left(\Pi_\sigma^2(x) + \frac{1}{g_\sigma^2} [\partial_x \vartheta_\sigma(x)]^2 \right), \end{aligned} \quad (4)$$

where v_σ is defined below and

$$g_\sigma = \left(\frac{1 + \eta_{\text{ex}}}{1 - \eta_{\text{ex}}} \right)^{1/2}, \quad (5)$$

with the exchange interaction matrix element $\eta_{\text{ex}} \equiv \hat{V}(2k_F)/2\pi\hbar v_F$. In Eq. (4), the electrons are represented by conjugate bosonic fields Π_ρ, ϑ_ρ , and $\Pi_\sigma, \vartheta_\sigma$ associated with the collective charge and spin density excitations, respectively. The system length is L and the Fermi velocity v_F . The interaction, $V(x-x')$, is a projection of a modified 3D Coulomb interaction onto the x direction (see below). It has the Fourier transform $\hat{V}(q)$, which is the dominant quantity in the dispersion relation of the charge excitations³³

$$\omega_\rho(q) = v_F |q| \left[1 - \eta_{\text{ex}}^2 + (1 + \eta_{\text{ex}}) \frac{2\hat{V}(q)}{\pi\hbar v_F} \right]^{1/2} \equiv v_\rho(q) |q|. \quad (6)$$

The dispersion relation of the spin excitations,

$$\omega_\sigma(q) = v_F |q| [1 - \eta_{\text{ex}}^2]^{1/2} \equiv v_\sigma |q|, \quad (7)$$

contains as the dominant part the exchange interaction, which is generally very small compared with $\hat{V}(q)$ at small q .^{25,33} This implies that the group velocity of the spin exci-

tations, v_σ , is very close to the Fermi velocity, $g_\sigma \approx 1$. In the following, η_{ex} will therefore be omitted whenever it is only a small correction.

The contribution of the two localized impurities is

$$H_B = \rho_0 \sum_{i=1,2} V_i \cos[2k_F x_i + \sqrt{2\pi} \vartheta_\rho(x_i)] \cos[\sqrt{2\pi} \vartheta_\sigma(x_i)], \quad (8)$$

where $\rho_0 = 2k_F/\pi$ is the mean electron density. Equation (8) is the potential energy of the impurities corresponding to the number density of charges:

$$\begin{aligned} \rho(x) &= \rho_\uparrow(x) + \rho_\downarrow(x) \\ &= \rho_0 + \sqrt{\frac{2}{\pi}} \partial_x \vartheta_\rho(x) + \rho_0 \cos[2k_F x + \sqrt{2\pi} \vartheta_\rho(x)] \\ &\quad \times \cos[\sqrt{2\pi} \vartheta_\sigma(x)]. \end{aligned} \quad (9)$$

The second term in Eq. (9) accounts for the slowly varying part of the charge fluctuations. The third term represents the charge density wave involved in the $2k_F$ backscattering interference between left and right moving electrons. It also couples the charge with the long-wavelength part of the density of spins,

$$\rho_\uparrow(x) - \rho_\downarrow(x) \approx \sqrt{\frac{2}{\pi}} \partial_x \vartheta_\sigma(x), \quad (10)$$

which is considered here with respect to a zero mean value. When calculating the energy of the impurities, one obtains also a contribution due to the second term in Eq. (9), besides the above contribution H_B . As this represents a forward scattering process, it can be eliminated by a unitary transformation and will not be considered any further.

On the other hand, if a potential is slowly varying on the scale k_F^{-1} , its dominant contribution is mainly due to the long-wavelength part of the density (9). We assume this to be the case for the bias electric field. The corresponding term in the Hamiltonian is, with the elementary charge e (>0),

$$H_U = -e \sqrt{\frac{2}{\pi}} \int dx U(x, t) \partial_x \vartheta_\rho(x). \quad (11)$$

The presence of the two localized impurities naturally separates the charge and spin degrees of freedom at ‘‘bulk’’ positions $x \neq x_1, x_2$ from those at the barriers. It is useful to introduce symmetric and antisymmetric variables for particle ($\nu = \rho$) and spin densities ($\nu = \sigma$):

$$N_\nu^\pm = \sqrt{\frac{2}{\pi}} [\vartheta_\nu(x_2) \pm \vartheta_\nu(x_1)]. \quad (12)$$

The quantity N_ρ^- is associated with the fluctuations of the particle number within the island as compared to the mean particle number $n_0 = \rho_0(x_2 - x_1)$. The corresponding excess charge is $Q = -eN_\rho^-$; N_σ^- represents the z component of the fluctuation of the number of spins within the island corresponding to a change of spin $N_\sigma^-/2$. The numbers of imbalanced particles and spins between left and right leads are represented by N_ν^+ . The dc current-voltage characteristic can

then be evaluated by considering the stationary limit of the charge transfer through the dot in the presence of an external voltage:

$$I = \frac{e}{2} \lim_{t \rightarrow \infty} \langle \dot{N}_\rho^+(t) \rangle. \quad (13)$$

The brackets $\langle \dots \rangle$ include a thermal average over the collective excitations at $x \neq x_1, x_2$ and a statistical average performed with the reduced density matrix for the degrees of freedom at $x = x_1, x_2$.

B. The interaction energy

We consider in the following two models which can be used for discussing experimental results quantitatively.

1. Model 1

Because of gates and surrounding charges in the experiments done on quantum wire, screening is always present for the interaction between the electrons which normally interact via the 3D Coulomb interaction. Although the geometry of the gates and the wire are certainly more difficult in the experiment,¹⁵ we assume in the following that we can describe the screening as being solely due to an infinite metallic plane at a distance D in the y -direction parallel to the (x, z) plane. The quantum wire is assumed in the x direction. The effective electron-electron interaction energy can then be calculated by using the method of image charges:

$$\begin{aligned} V(\vec{r} - \vec{r}') &= \frac{V_0}{|\vec{r} - \vec{r}'|} - \frac{V_0}{\sqrt{(x - x')^2 + (z - z')^2 + (y + y' - 2D)^2}}, \end{aligned} \quad (14)$$

with $V_0 = e^2/4\pi\epsilon_0\epsilon$ and the dielectric constant $\epsilon_0\epsilon$.

We assume for simplicity a parabolic confinement of the electrons perpendicular to the wire. The effective interaction in the lowest subband can then be obtained from Eq. (14) by projecting with a normalized Gaussian confinement wave function corresponding to the diameter d of the wire. The Fourier transform of the resulting effective interaction potential is for $D \gg d$

$$\hat{V}(q) = V_0 \left[e^{d^2 q^2/4} E_1\left(\frac{d^2 q^2}{4}\right) - 2K_0(2Dq) \right], \quad (15)$$

where $E_1(z)$ is the exponential integral and $K_0(z)$ the modified Bessel function.³⁴ This expression shows explicitly how the gate screens the Coulomb interaction. In the limit $qd \rightarrow 0$, one obtains the finite value $\hat{V}(q \rightarrow 0) = 2V_0[\gamma/2 + \ln(2D/d)]$ ($\gamma = 0.57722$ Euler constant). This implies a finite interaction constant

$$g_\rho \equiv \frac{v_F}{v_\rho(q \rightarrow 0)} = \left[1 + \eta\gamma + 2\eta \ln\left(\frac{2D}{d}\right) \right]^{-1/2}, \quad (16)$$

where $\eta = 2V_0/\pi\hbar v_F$. The 1D equivalent of the unscreened Coulomb interaction is obtained for $D \rightarrow \infty$.

2. Model 2

We also consider the screened Coulomb interaction

$$V(\vec{r}-\vec{r}') = V_0 \frac{e^{-\alpha|\vec{r}-\vec{r}'|}}{|\vec{r}-\vec{r}'|}, \quad (17)$$

with a phenomenological screening length α^{-1} . The Fourier transform of its Gaussian projection to 1D is¹⁰

$$\hat{V}(q) = V_0 e^{(d^2/4)(q^2 + \alpha^2)} E_1 \left(\frac{d^2}{4} [q^2 + \alpha^2] \right), \quad (18)$$

and the corresponding interaction constant

$$g_\rho = \left[1 - \eta\gamma + 2\eta \ln \left(\frac{2}{\alpha d} \right) \right]^{-1/2}. \quad (19)$$

III. THE EFFECTIVE ACTION

In order to evaluate the current-voltage characteristic one has to perform a thermal average over the ‘‘bulk modes’’ at $x \neq x_1, x_2$. This can be done with the imaginary-time path integral method.³⁵ The result of the integration is an effective action S_{eff} , which depends only on the four variables defined in Eq. (12). In the continuous limit ($L \rightarrow \infty$), with the inverse temperature $\beta = 1/k_B T$ one obtains

$$\begin{aligned} S_{\text{eff}}[N_\rho^\pm, N_\sigma^\pm] &= \int_0^{\hbar\beta} d\tau H_B[N_\rho^\pm, N_\sigma^\pm] \\ &+ \sum_{r=\pm} \sum_{\nu=\rho,\sigma} \left[\int_0^{\hbar\beta} \int_0^{\hbar\beta} d\tau d\tau' N_\nu^r(\tau) K_\nu^r(\tau-\tau') \right. \\ &\left. \times N_\nu^r(\tau') - \delta_{\rho,\nu} \int_0^{\hbar\beta} d\tau N_\rho^r(\tau) \mathcal{L}^r(\tau) \right]. \quad (20) \end{aligned}$$

The Fourier transforms, at Matsubara frequencies $\omega_n = 2\pi n/\hbar\beta$, of the dissipative kernels $K_\nu^\pm(\tau)$ and of the effective ‘‘forces’’ $\mathcal{L}^\pm(\tau)$ are determined by the dispersion relations (6) and (7) of the collective modes, respectively,

$$[K_\nu^\pm(\omega_n)]^{-1} = \frac{8v_\nu g_\nu}{\hbar \pi^2} \int_0^\infty dq \frac{1 \pm \cos[q(x_1 - x_2)]}{\omega_n^2 + \omega_\nu^2(q)}, \quad (21)$$

$$\begin{aligned} \mathcal{L}^\pm(\omega_n) &= \frac{4e v_F}{\hbar \pi^2} K_\rho^\pm(\omega_n) \int_{-\infty}^\infty dx \mathcal{E}(x, \omega_n) \\ &\times \int_0^\infty dq \frac{\cos[q(x-x_2)] \pm \cos[q(x-x_1)]}{\omega_n^2 + \omega_\rho^2(q)}. \quad (22) \end{aligned}$$

Both K_ν^\pm and \mathcal{L}^\pm contain the collective bulk modes that introduce the interaction effects to be described below. First of all, we note that $K_\nu^+(\omega_n \rightarrow 0) = 0$.^{21,35} On the other hand, $K_\nu^-(\omega_n \rightarrow 0) \neq 0$. The latter describe the costs in energy for

changing the numbers of charges and/or spins on the island between the potential barriers. The corresponding Euclidean action is

$$S_0[N_\rho^-, N_\sigma^-] = \sum_{\nu=\rho,\sigma} \frac{E_\nu}{2} \int_0^{\hbar\beta} d\tau (N_\nu^-)^2, \quad (23)$$

with the characteristic energies

$$E_\nu = 2K_\nu^-(\omega_n \rightarrow 0) \quad (\nu = \rho, \sigma). \quad (24)$$

For $\nu = \rho$, this corresponds to the charging energy that is supplied or gained, in order to transfer or remove one charge to or from the island as compared with the mean value, $N_\rho^- = \pm 1$. Correspondingly, for $\nu = \sigma$, the spin addition energy E_σ is needed or gained in order to change the spin by exactly $\pm 1/2$. The Coulomb interaction in the dispersion relation of the charge excitations increases considerably the charging energy E_ρ , in comparison with the spin addition energy E_σ , which is only influenced by the (small) exchange interaction. We always expect $E_\rho > E_\sigma$.

The frequency-dependent parts of the kernels describe the dynamical effects of the external leads and of the correlated excited states in the dot. Their influence is described by spectral densities $J_\nu^\pm(\omega)$ related via analytic continuation to the imaginary-time kernels^{20,36}

$$J_\nu^\pm(\omega) = \frac{2}{\pi\hbar} \text{Im} K_\nu^\pm(\omega_n \rightarrow i\omega). \quad (25)$$

Due to the nonzero range of the interaction, analytic expressions for these densities are not available. However, one can always extract their limits for $\omega \rightarrow 0$,

$$J_\nu^\pm(\omega \rightarrow 0) = \frac{A_\nu^\pm(g_\nu)}{4g_\nu} \omega, \quad (26)$$

where $A_\rho^- = g_\rho^4 (E_\rho/E_0)^2$ ($E_0 = \hbar \pi v_F/2a$), and for the three other combinations of indices $A_\nu^\pm = 1$. This limit describes the dissipative influence of the low-frequency charge and spin excitations in the external leads, $x < x_1$ and $x > x_2$. It holds also for finite frequencies. However, these must be smaller than the frequency scale corresponding to the range of the interaction, and smaller than the characteristic excitation energy of the correlated electrons in the dot.

Let us now discuss the driving forces. In general, $\mathcal{L}^\pm(\tau)$ depend in a quite complicated way on the dispersion of the collective modes and on the shape of the electric field. We focus on the dc limit where it is sufficient to evaluate the Fourier components for $\omega_n \rightarrow 0$. In this case, the quantity $\mathcal{L}^+(\tau)$, which acts on the total transmitted charge, depends only on the integral of the time-independent electric field over the entire system, the source-drain voltage $U \equiv \int_{-\infty}^\infty dx \mathcal{E}(x)$,

$$\mathcal{L}^+(\tau) = \frac{eU}{2}. \quad (27)$$

Since \mathcal{L}^+ is the part of the effective force that generates the current transport, this result generalizes the one obtained previously for only one impurity.³⁵ It can be easily derived from Eq. (22) by using the relation

$$\frac{e^2 v_F}{\hbar \pi^2} \int_0^\infty dq \frac{\omega_n (1 \pm \cos qx)}{\omega_n^2 + \omega_\rho^2(q)} = \sigma_0(0, \omega_n) \pm \sigma_0(x, \omega_n). \quad (28)$$

Here, $\sigma_0(x, \omega_n)$ is the frequency dependent nonlocal conductivity of the Luttinger liquid per spin channel³⁵ with the dc limit $\sigma_0(x, 0) = g_\rho e^2/h$.

On the other hand, $\mathcal{L}^-(\tau)$ acts on the excess charge on the island; it does *not* generate a current. It depends on the spatial shape of the electric field and can formally be written in terms of the total charge $Q_\mathcal{E}$ accumulated between the points x_1 and x_2 in the absence of the barriers as a consequence of the presence of the dc electric field

$$\mathcal{L}^-(\tau) = \frac{E_\rho Q_\mathcal{E}}{e}, \quad (29)$$

where the charge is given by

$$Q_\mathcal{E} = 2 \int_{-\infty}^\infty dx' \mathcal{E}(x') \times \lim_{\omega \rightarrow 0} \left[\frac{\sigma_0(x_1 - x', -i\omega) - \sigma_0(x_2 - x', -i\omega)}{i\omega} \right]. \quad (30)$$

Equivalently, this can also be understood in terms of addition energies. By introducing explicitly in Eqs. (22) and (24) the dependence on the interval considered when evaluating the addition energies, one finds

$$\mathcal{L}^-(\tau) = \frac{e}{2} E_\rho (x_1 - x_2) \int_{-\infty}^\infty dx \mathcal{E}(x) \times \left[\frac{1}{E_\rho(x-x_1)} - \frac{1}{E_\rho(x-x_2)} \right]. \quad (31)$$

It is reasonable to assume $x_{2,1} = \pm a/2$. If the effective electric field has inversion symmetry, \mathcal{L}^- vanishes. Without inversion symmetry, the electric field generates an effective charge on the island that will influence the total current via coupling between N_ρ^+ and N_ρ^- due to the impurity Hamiltonian H_B . Physically, this externally induced charge may be thought of as being generated by a voltage V_G applied to an external gate that electrostatically influences the charge on the island. Thus, the above Eq. (29) can be interpreted as a term representing the effect of the gate voltage in the phenomenological theory of the Coulomb blockade.

IV. CONDITIONS FOR CURRENT TRANSPORT

So far, we have discussed the influence of the spin and charge bulk modes on the four variables N_ν^\pm that describe the quantum dot. In order to calculate explicitly the electrical current one has to solve the equations of motion for the N_ν^\pm . This is beyond the scope of the present work and will be discussed elsewhere. Here, we briefly describe the results that are needed in the following.

For barriers much higher than the charging energy, $V_i \gg E_\rho$, the dynamics is dominated by tunneling events connecting the minima of H_B in the 4D $(N_\rho^+, N_\rho^-, N_\sigma^+, N_\sigma^-)$

space.⁷ For equal barriers, $V_1 = V_2 = V$, the impurity Hamiltonian is

$$H_B = \rho_0 V \left[\cos \frac{\pi N_\rho^+}{2} \cos \frac{\pi N_\sigma^+}{2} \cos \frac{\pi(n_0 + N_\rho^-)}{2} \cos \frac{\pi N_\sigma^-}{2} + \sin \frac{\pi N_\rho^+}{2} \sin \frac{\pi N_\sigma^+}{2} \sin \frac{\pi(n_0 + N_\rho^-)}{2} \sin \frac{\pi N_\sigma^-}{2} \right]. \quad (32)$$

The transitions between the minima of this function of four variables correspond to different physical processes of transferring electrons from one side to the other of the quantum dot. At very low temperature, the dominant processes transfer the electron coherently through the dot. In particular, when the number of particles in the island is an odd integer there is spin degeneracy, $N_\sigma^- = \pm 1$. The island acts as a localized magnetic impurity, similar to that in the Kondo effect.⁷ This leads to a Kondo resonance in the transport through the island.^{37,38}

On the other hand, if the temperature is higher than the tunneling rate through the single barrier, the dominant processes are sequential tunneling events.^{19,21} The transfer of charge occurs via uncorrelated single-electron hops into and out of the island, associated with corresponding changes in the total spin. This is precisely the regime that recently has become accessible by using cleaved-edge-overgrowth quantum wires.¹⁵ In this region, one has to consider minima that correspond to pairs of even or odd N_ρ^- and N_σ^- . The dominant transport processes are those that connect minima via transitions $N_\rho^- \rightarrow N_\rho^- \pm 1$ associated with changes of the spin $N_\sigma^- \rightarrow N_\sigma^- \pm 1$. For each of these processes also the external charge and the spin change by $N_\nu^+ \rightarrow N_\nu^+ \pm 1$.

The degeneracy of these minima is lifted by the charge and spin addition energies E_ρ and E_σ , which force the system to select favorable charge and spin states in the island. These selections become essential at low temperatures, $k_B T < E_\nu$, when current can flow only under resonant conditions. The latter can be achieved in experiment by tuning external parameters, like the source-drain voltage or the gate voltage, in order to create degenerate charge states in the island.

A. Linear transport

In the linear regime, $U \rightarrow 0$ for $T=0$, starting with the island occupied by n electrons, we expect that another electron can enter and leave only if the difference between the ground-state energies of $n+1$ and n electrons are aligned with the chemical potential of the external semi-infinite Luttinger systems. The ground state of an even number of electrons in the 1D island has the total spin 0. On the other hand, the ground state of an odd number of electrons can be assumed to have the spin $N_\sigma^- = \pm 1$.^{24,39} This implies the resonance condition

$$\mathcal{U}(n+1, \pm s_{n+1}) - \mathcal{U}(n, \pm s_n) = 0 \quad (33)$$

with $\mathcal{U}(n, \pm s_n)$ the ground-state energies with n particles and total spins $s_n = 0$ (n even) or $s_n = 1/2$ (n odd), respectively.

With the above charge, spin, and external gate terms, Eqs. (24) and (29), these conditions become

$$E_\rho \left(n - n_0 - n_G + \frac{1}{2} \right) + (-1)^n \frac{E_\sigma}{2} = 0. \quad (34)$$

The variable $n_G = eV_G \delta / E_\rho$ represents the number of induced particles due to the coupling to a gate at which the voltage V_G is applied, with a proportionality factor δ that can be determined experimentally. The zero of energy has been assumed to be given by the external chemical potential in Eq. (33).

From the above expression one can see that the distance of the peaks of the linear conductance when changing the gate voltage is given by $\Delta V_G = [E_\rho + (-1)^n E_\sigma] / e\delta \approx E_\rho / e\delta$ since $E_\sigma \ll E_\rho$. Having independent information on δ one can extract the value of the charging energy E_ρ (in principle also for the spin addition energy E_σ) from the experimental data.

In order to evaluate the current as a function of temperature and/or source-drain voltage, one needs to consider the behavior of the spectral densities given in Eq. (25). In the sequential tunneling regime, one can show that only their sum enters the transport²¹

$$J(\omega) = \sum_{r=\pm} \sum_{\nu=\rho,\sigma} J_\nu^r(\omega). \quad (35)$$

The frequency behavior of this determines the current-voltage characteristics both in the linear and in the nonlinear regimes (see below). In particular, it determines the exponent of the power-law dependencies of the current as a function of temperature and/or the bias voltage.

For temperatures lower than the excitation energy in the quantum dot, the low-frequency behavior of the spectral density is mainly determined by the charge and spin excitations in the leads. Thus, the power-law dependence of the conductance peaks is dominated by the interaction in the regions of the quantum wire *outside* of the electron island. From Eqs. (25) and (26) one obtains

$$J(\omega) \approx J_{\text{leads}}(\omega) = \frac{\omega}{2} \left(\frac{1}{g_\sigma} + \frac{1 + A_\rho^-}{2g_\rho} \right). \quad (36)$$

Equation (36) generalizes the results obtained previously for spinless electrons and zero-range interaction,^{19,21} where $J(\omega) \approx \omega/g_\rho$. We conclude that the presence of the spin in the leads introduces an effective interaction strength

$$\frac{1}{g_{\text{eff}}} = \frac{1}{4} \left(\frac{1 + A_\rho^-}{g_\rho} + \frac{2}{g_\sigma} \right), \quad (37)$$

which determines the exponents of the power laws.

For example, it has been shown for spinless electrons^{19,21} that the intrinsic width $\Gamma(T)$ of the linear conductance Coulomb peak depends on the temperature. For low temperatures this has been found to be given by $\Gamma(T) \propto T^{1/g_\rho - 1}$. Correspondingly, with spin, one finds instead

$$\Gamma(T) \propto T^{1/g_{\text{eff}} - 1}. \quad (38)$$

B. Nonlinear transport

One can investigate the nonlinear current-voltage characteristic by increasing the source-drain voltage U . In this case, the current-voltage characteristic shows the Coulomb stair-

case associated with transitions between successive ground states of the electrons in the quantum dot. In addition, fine structure appears that reflects the excitation spectra of the correlated electrons. They can be due to collective charge and spin modes or to particular polarizations of the spins, $N_\sigma^- \neq 0, \pm 1$. The former, for a voltage drop U at the potential barriers (fixing the chemical potential in one of the leads to be equal to that in the dot), has a maximum periodicity

$$U = \mu_0(n+1) - \mu_0(n) = E_\rho + (-1)^{n+1} E_\sigma, \quad (39)$$

where $\mu_0(n)$ is the electrochemical potential of n electrons on the quantum island.

In the present model, the possible particle-hole excitations are collective spin and charge modes confined within the island. In a completely isolated island, the corresponding energy spectrum would be discrete, $\omega_\rho(q_m)$ and $\omega_\sigma(q_m)$, due to the discretization of the wave number $q_m = \pi m/a$ associated with the confinement. Due to the coupling to the electrons in the leads via the interaction, these levels are broadened. In the following argument, we assume that this broadening is negligible.

The screened Coulomb interaction causes a nonlinear dispersion relation for the charge modes in the infinite Luttinger system. This leads to nonequidistant charge excitation energies in the quantum dot,

$$\Delta \epsilon_\rho(q_m) = \hbar [\omega_\rho(q_{m+1}) - \omega_\rho(q_m)]. \quad (40)$$

Their explicit values depend on the ratio between the distance a and the range of the interaction, D or α^{-1} .

For values of a much larger than this range, the first excited charge modes are equidistant. They are given by the charge-sound velocity for $q \rightarrow 0$, $v_\rho = v_F/g_\rho$,

$$\Delta \epsilon_\rho = \frac{\hbar \pi v_\rho}{a} = \frac{\hbar \pi v_F}{a g_\rho} \equiv \frac{2E_0}{g_\rho}. \quad (41)$$

In the opposite limit, the nonlinear dispersion is already affecting strongly the first excitation. This results in a value smaller than Eq. (41), for model 1,

$$\Delta \epsilon_\rho = \frac{\hbar \pi v_F}{a} \sqrt{1 - \gamma \eta + 2 \eta \ln \left(\frac{2a}{\pi d} \right)} \equiv \frac{2E_0}{f_\rho}. \quad (42)$$

For the spin excitations, the dispersion in the infinite system is linear and the discrete spectrum is equidistant,

$$\Delta \epsilon_\sigma = \frac{\hbar \pi v_\sigma}{a} \equiv 2E_0 \frac{v_\sigma}{v_F}, \quad (43)$$

with the spin mode velocity v_σ ($\approx v_F$).

V. THE CHARGING ENERGY

The above discussion emphasizes the *importance of charge and spin addition energies* and of the *charge and spin excitation energies* for the linear and nonlinear transport properties. It is therefore crucial to evaluate these quantities microscopically and determine their dependencies on the model parameters, especially in view of comparisons with the experimental data of Ref. 15.

We analyze now in more detail the charging and spin energies of the Luttinger island as a function of the param-

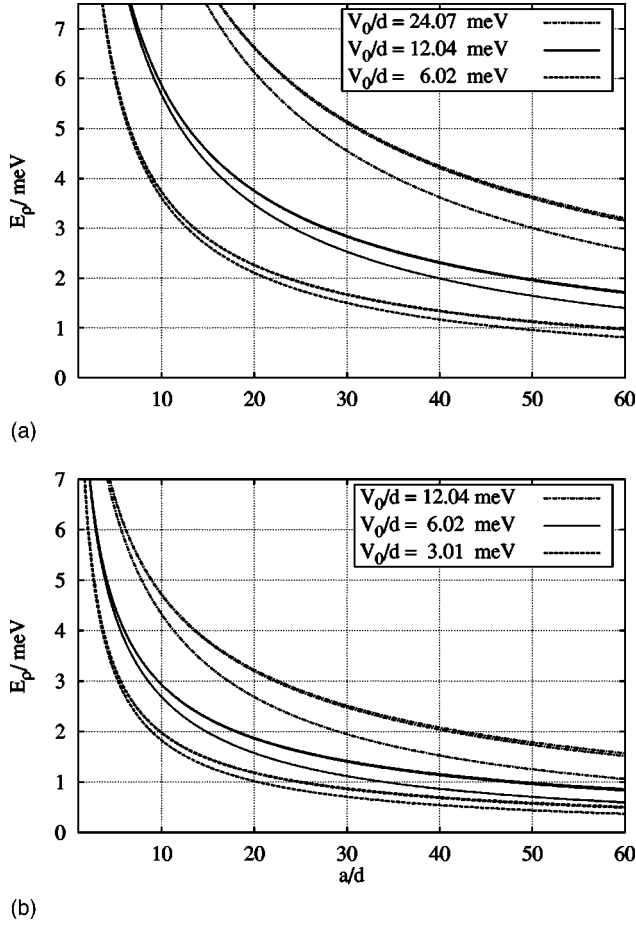


FIG. 1. Charging energy E_ρ in meV for model 1 as a function of a/d (Fermi energy $E_F=3$ meV, effective electron mass $m=0.067m_0$). Top: $d=10$ nm; interaction strengths $V_0/d=24.08$ meV (dashed-dotted), 12.04 meV (full lines), 6.02 meV (dotted lines), corresponding to $\epsilon=6, 12, 24$ (equivalent to $\eta=2V_0/\pi\hbar v_F=2.04, 1.02, 0.51$, respectively), and $D/d=1000, 100, 10$ (top to bottom). Bottom: $d=20$ nm; interaction strengths $V_0/d=12.04$ meV (dashed-dotted lines), 6.02 meV (full lines), 3.01 meV (dotted lines), and $D/d=500, 50, 5$ (top to bottom).

eters of the above model 1. In addition to the interaction strength V_0 , which contains as an essential quantity the dielectric constant ϵ , we have the Fermi energy E_F and three geometrical parameters: the distance D between the 1D system and the infinite metallic plane, the diameter d of the wire, and the length a of the island.

The spin addition energy can be easily evaluated from the simple dispersion relation Eq. (7),

$$E_\sigma = \frac{\pi\hbar v_\sigma}{2a g_\sigma}. \quad (44)$$

This energy is the same as the addition energy of noninteracting particles that is related to the Pauli principle and due to the quasidiscretization of the spin energies in the dot.

The charging energy E_ρ is evaluated numerically from Eq. (24) as a function of a/d . It is shown in Fig. 1 for different ratios D/d and different interaction parameters V_0/d with $d=10$ nm and $d=20$ nm. Different V_0/d correspond to different ϵ . Changing E_F between 2 meV and 4 meV, values that cover the experimentally relevant region,

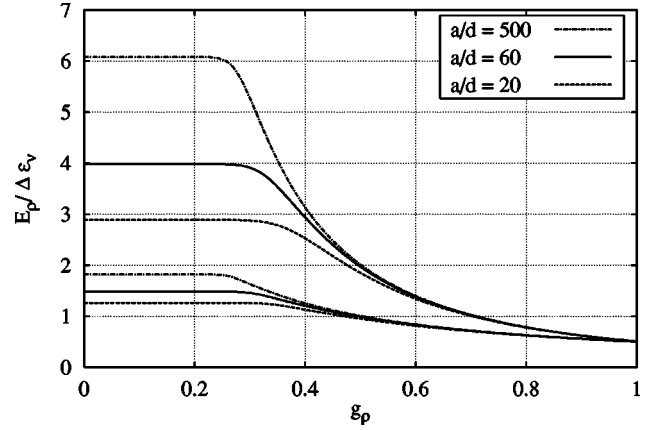


FIG. 2. Ratios $E_\rho/\Delta\epsilon_\nu$ ($\nu=\sigma,\rho$; upper/lower curves for fixed a/d) as a function of the interaction constant g_ρ for $a/d=20, 60, 500$ with $\epsilon=12$, $d=20$ nm, $m=0.067m_0$, $g_\sigma=1$.

changes the curves in Fig. 1 only less than 10%. For small a/d , the charging energy diverges. We consider only the region $a/d>1$. Asymptotically,

$$\frac{E_\rho}{E_0} \approx \begin{cases} \left[1 + \eta\gamma + 2\eta \ln\left(\frac{2D}{d}\right) \right] \equiv \frac{1}{g_\rho^2} & (D \ll a), \\ \left[1 - \eta\gamma + 2\eta \ln\left(\frac{2a}{\pi d}\right) \right] \equiv \frac{1}{f_\rho^2} & (D \gg a). \end{cases} \quad (45)$$

E_ρ is only weakly influenced by D/d : changing D/d by 2 orders of magnitude changes E_ρ only by about 30%.

The charging energy always increases with increasing interaction range D , because the cost of energy for putting additional electrons into the island increases. Interaction ranges much larger than a do not change the charging energy because only the short-range part of the repulsion between the electrons contributes. Therefore, E_ρ approaches the asymptotic value of Eq. (46) (Fig. 1, curves for largest D/d). For strong Coulomb interaction ($\eta=2V_0/\pi\hbar v_F \gg 1$) and $a \gg d$, this is

$$E_\rho = \frac{e^2}{2\pi\epsilon\epsilon_0 a} \ln\left(\frac{2a}{d}\right) \equiv \frac{e^2}{C}. \quad (47)$$

Here, C is the classical self-capacitance of a cylinder of the length a . The stronger the interaction (increasing V_0) the larger the E_ρ , very similar to the behavior of a classical capacitor with a dielectric, $C \propto \epsilon$.

Very similar results, with d/D replaced by ad , are obtained by using model 2. Basically, this tells that screening effects may well be described by a global parameter, irrespective of the underlying microscopic model.

As mentioned earlier, the nonlinear transport shows Coulomb steps with widths given approximately by E_ρ and fine structure due to the excited states. For a first estimate of the strength of the interaction it is very useful to estimate how many excited states are present within the energy window given by E_ρ . Figure 2 shows the ratios between the energy E_ρ and the first collective excited (spin or charge) state in the electron island $\Delta\epsilon_\nu$ ($\nu=\sigma,\rho$) for model 1 as a function of the interaction constant g_ρ . The change in g_ρ is obtained

changing the distance D from the gate; $g_\rho \rightarrow 0$ corresponds to $D \rightarrow \infty$. The ratio $E_\rho/\Delta\epsilon_\rho$ is always smaller than $E_\rho/\Delta\epsilon_\sigma$.

We expect to observe within the window E_ρ much more levels due to spin excitations than due to charge excitations; $E_\rho/\Delta\epsilon_\nu$ always increases when g_ρ decreases (increasing D). It saturates for $D \gg a$,

$$\frac{E_\rho}{\Delta\epsilon_\rho} = \frac{1}{2f_\rho}; \quad \frac{E_\rho}{\Delta\epsilon_\sigma} = \frac{v_F}{v_\sigma} \frac{1}{2f_\rho^2}. \quad (48)$$

In the opposite limit, $D \ll a$, the behavior is described by the asymptotic expressions

$$\frac{E_\rho}{\Delta\epsilon_\rho} = \frac{1}{2g_\rho}; \quad \frac{E_\rho}{\Delta\epsilon_\sigma} = \frac{v_F}{v_\sigma} \frac{1}{2g_\rho^2}. \quad (49)$$

VI. COMPARISON WITH EXPERIMENT

In this section, we compare our results with the experimental data obtained in Ref. 15. In that work, results of the temperature dependence of the intrinsic width of the conductance peaks in the region of Coulomb blockade on quantum wires fabricated with the cleaved-edge-overgrowth technique have been reported. The data have been found to be consistent with the power law

$$\Gamma(T) \propto T^{1/g^*-1}, \quad (50)$$

with $g^* \approx 0.82$ and $g^* \approx 0.74$ for a peak closer to the onset of the conductance and the next lower peak, respectively. In addition, information about the excited energy levels of correlated electrons have been obtained by measuring the nonlinear current-voltage characteristics. A *minimum* of five excited levels have been observed for a given electron number. Presumably, the number of excited levels is even larger since the majority of the excited island states is generally not clearly observed in nonlinear transport due to matrix element effects.⁴⁰

The data have been analyzed previously by assuming that within the quantum wire, a quantum dot has been accidentally formed between two maxima of the random potential of impurities. The electron spin has been neglected. The parameters estimated from the experimental setup are length of wire $L \approx 5 \mu\text{m}$; length of the electron island $a \approx 100\text{--}200 \text{ nm}$; (nonspherical) diameter of the wire $d \approx 10\text{--}25 \text{ nm}$; distance to the gate $D \approx 0.5 \mu\text{m}$. The charging energy, as estimated from the distance between the conductance peaks, has been given as $E_C \approx 2.2 \text{ meV}$. Since the observed conductance peaks are equidistant within 10% we deduce that $E_\sigma \ll E_\rho$. A rough estimate of the Fermi energy is $E_F \approx 3 \text{ meV}$. With these parameters, the value of the interaction constant has been estimated as $g_\rho \approx 0.4$,¹⁵ clearly inconsistent with the above g^* determined from the temperature dependence of the conductance peaks.

Using our above microscopic approach, which includes the influence of the electron spin and finite range of the interaction, we confirm that there is a discrepancy, though the estimate for g_ρ from the temperature dependence of the conductance peaks seems to be slightly improved. First, we estimate the length of the island a from the charging energy in Fig. 1. As E_ρ is relatively insensitive with respect to changes

of D/d and E_F in the experimentally relevant region of parameters, we assume $D/d = 50$ with $E_F = 3 \text{ meV}$ and $d = 20 \text{ nm}$. Furthermore, $V_0/d = 6.02 \text{ meV}$ for $\epsilon = 12$. With the above 2.2 meV we find $a/d \approx 16$. This is consistent with the value given in Ref. 15 within the uncertainties.

By taking into account the spin and using an interaction of a finite range, g^* has to be identified with the effective interaction g_{eff} in Eq. (37). Since for the spin excitations $g_\sigma \approx 1$, we find for $g^* = 0.82$ and 0.74 an interaction constant $g_\rho^* \approx 0.6 \pm 20\%$ by solving Eq. (37) for $E_\rho(g_\rho)/E_0$ and comparing with $E_\rho(g_\rho)/2E_0 = E_\rho/\Delta\epsilon_\sigma$ in Fig. 2. This would imply that $D \approx d$ [Eq. (16)]. On the other hand, by using Eq. (16) with the above parameters, especially $D \approx 50d$, we find an interaction constant $g_\rho \approx 0.25 \pm 20\%$ depending only weakly on D/d . This is clearly *not* a quantitatively consistent result. The discrepancy can be reduced by changing ϵ . Also, taking into account the exchange correction η_{ex} ($g_\sigma \neq 1$) gives some improvement. However, within reasonable values of all of the parameters, one is in any case forced to conclude $g_\rho^* \approx 2g_\rho$.

Furthermore, with $g_\rho^* = 0.6$, one reads from Fig. 2 $E_\rho/\Delta\epsilon_\rho \approx E_\rho/\Delta\epsilon_\sigma \approx 1$. Thus, about one to two excited states corresponding to a given electron number should be observed in nonlinear transport spectroscopy. This is also *not* consistent with the experiment. In order to observe a larger number of excited states, the interaction constant must be considerably smaller, $g_\rho < 0.3$, such that the number of spin excited states within the given window of E_ρ is increased (cf. Fig. 2). Taking into account the exchange interaction ($v_\sigma < v_F$) would additionally decrease $\Delta\epsilon_\sigma$ (and E_σ) and increase E_ρ and thus increase the number of excited states.

Despite the above inconsistency, the energetically lowest of the excited states seen in the nonlinear transport are predicted by our approach to correspond to spin excitations. Without the latter there is not at all any possibility of understanding the results from nonlinear transport even when using parameters that give consistent results for the interaction constants. Given this scenario, only the energetically highest experimentally observed state would correspond to a charge excitation. The latter could be identified, for instance, with the state denoted in Ref. 15 as the ‘‘strongly coupled excited state.’’

One might conclude that the part of above quantitative discrepancy is due to the Luttinger model being questionable for quantum wires in the extreme low-density limit. However, one can also conclude that the data obtained from nonlinear transport *spectroscopy* have to be interpreted by using a different interaction constant than that obtained from the temperature dependence of the transport. This is also supported by the theoretical derivation: the temperature behavior of the conductance peaks is dominated by the excitations in the whole quantum wire, while the quasidiscrete excitation spectra are showing the interaction in the region of the quantum island. We are thus forced to conclude that *inhomogeneity* effects and the influence of the contacts are an important issue for the understanding of the correlations in the electron transport in these cleaved-edge-overgrowth quantum wires, in addition to spin effects.

VII. CONCLUSION

In conclusion, we have derived the effective action for a quantum dot formed by a double-barrier potential with a re-

alistic long-range interaction between the electrons, and, most importantly, including the electron spin. We have identified an effective driving force acting on the charge of the electrons, which turned out to be independent of the shape of the driving electric field. Mass terms originating from the dissipative degrees of freedom in the Luttinger liquid have been found for both the charge *and the spin*. They are identified with the charging energy in the case of the addition of charge and with a spin addition energy for the spin. Also, an effective force has been found, which, in the dc limit, is only nonzero when the driving electric field and/or the barriers are asymmetric. This influences the transport via the coupling of modes at the potential barriers. It can be attributed to charging of the electron island via an external gate.

We have made an attempt to interpret quantitatively a recent experiment that includes linear as well as nonlinear transport data in the region of the Coulomb blockade. We find that even taking into account the electron spin it is impossible to consistently fit *all* of the experimental data with the same interaction parameter. It seems that different interaction strengths have to be used for explaining the temperature dependence of the transport on the one hand and the excitation spectrum of the quantum dot on the other.

A possible conjecture to solve this puzzle is to assume that the temperature behavior of the conductance peaks is dominated by the interaction among the electrons in the quantum wire along the edge of the whole sample, in contrast to the excitation spectra that “feel” the interaction strength near the quantum dot. This is qualitatively consistent with the physical origin of the temperature dependence of the conductance, namely, the bulk modes outside the elec-

tron island. This conjecture would also explain why $g_{\rho}^* \approx 0.6$, as estimated from the temperature behavior, is larger than that obtained from the observed number of the excited states in the island, $g_{\rho} < 0.3$. The interaction is weaker in the leads due to screening induced by the contact regions with the attached 2D electron gases, while it can be assumed to be stronger within the island due to the absence of nearby 2D electron gases.

The above interpretation also predicts that the energetically lowest collective excitations in the quasi-1D quantum island observed in the experiment are very likely spin excitations. The energies of the lowest observed collective excited states are so small that it is hard to believe that they can be related to charge modes since $v_{\rho} > v_{\sigma}$, given the above estimates for the range and strength of the interaction is of the correct order. This is consistent with a previous suggestion based on a semiphenomenological model in which exact diagonalization and rate equations have been combined in order to describe the nonlinear transport through a 1D quantum island containing only few electrons.²⁴

ACKNOWLEDGMENTS

This work has been initiated at the 225th International WE-Heraeus Seminar in Bad Honnef, and has been supported by the European Union within the TMR program, by the

Deutsche Forschungsgemeinschaft within the SFB 508 of the Universität Hamburg, and by the Italian MURST via Cofinanziamento 98.

*Permanent address: I. Institut für Theoretische Physik, Universität Hamburg, Jungiusstraße 9, 20355 Hamburg, Germany.

¹S. Tarucha, T. Honda, and T. Saku, *Solid State Commun.* **94**, 413 (1995).

²A. Yacoby, H. L. Stormer, Ned S. Wingreen, L. N. Pfeiffer, K. W. Baldwin, and K. W. West, *Phys. Rev. Lett.* **77**, 4612 (1996).

³A. Yacoby, H. L. Stormer, K. W. Baldwin, L. N. Pfeiffer, and K. W. West, *Solid State Commun.* **101**, 77 (1997).

⁴S. Tomonaga, *Prog. Theor. Phys.* **5**, 544 (1950).

⁵J. M. Luttinger, *J. Math. Phys.* **4**, 1154 (1963).

⁶F.D.M. Haldane, *J. Phys. C* **14**, 2585 (1981).

⁷C. L. Kane and M. P. A. Fisher, *Phys. Rev. Lett.* **68**, 1220 (1992); *Phys. Rev. B* **46**, 15 233 (1992).

⁸A. Kawabata, *J. Phys. Soc. Jpn.* **65**, 30 (1995).

⁹Y. Oreg and A. Finkel'stein, *Phys. Rev. B* **54**, R14 265 (1996).

¹⁰G. Cuniberti, M. Sassetti, and B. Kramer, *Phys. Rev. B* **57**, 1515 (1998).

¹¹D. L. Maslov and M. Stone, *Phys. Rev. B* **52**, R5539 (1995).

¹²V. V. Ponomarenko, *Phys. Rev. B* **52**, R8666 (1995).

¹³I. Safi and H. J. Schulz, *Phys. Rev. B* **52**, R17 040 (1995).

¹⁴D. L. Maslov, *Phys. Rev. B* **52**, R14 368 (1995).

¹⁵O. M. Auslaender, A. Yacoby, R. de Picciotto, K. W. Baldwin, L. N. Pfeiffer, and K. W. West, *Phys. Rev. Lett.* **84**, 1764 (2000).

¹⁶D. V. Averin and K. K. Likharev, in *Mesoscopic Phenomena in Solids*, edited by B. L. Altshuler, P. A. Lee, and R. A. Webb (Elsevier, Amsterdam, 1991).

¹⁷U. Meirav, M. A. Kastner, and S. J. Wind, *Phys. Rev. Lett.* **65**, 771 (1990).

¹⁸L. P. Kouwenhoven, C. M. Marcus, P. L. McEuen, S. Tarucha, R. M. Westervelt and N. S. Wingreen, in *Mesoscopic Electron Transport*, NATO Advanced Studies Institute, Ser. E 345, edited by L. L. Sohn, G. Schön, and L. P. Kouwenhoven (Kluwer Academic, Dordrecht, 1997), p. 105.

¹⁹A. Furusaki, *Phys. Rev. B* **57**, 7141 (1998).

²⁰A. Furusaki and N. Nagaosa, *Phys. Rev. B* **47**, 3827 (1993).

²¹A. Braggio, M. Grifoni, M. Sassetti, and F. Napoli, *Europhys. Lett.* **50**, 136 (2000).

²²A. T. Johnson, L. P. Kouwenhoven, W. de Jong, N. C. van der Vaart, C. J. P. M. Harmans, and C. T. Foxon, *Phys. Rev. Lett.* **69**, 1592 (1992).

²³J. Weis, R. J. Haug, K. von Klitzing, and K. Ploog, *Phys. Rev. Lett.* **71**, 4019 (1993).

²⁴D. Weinmann, W. Häusler, and B. Kramer, *Phys. Rev. Lett.* **74**, 984 (1995); *Ann. Phys. (Leipzig)* **5**, 652 (1996).

²⁵M. Sassetti and B. Kramer, *Phys. Rev. Lett.* **80**, 1485 (1998); *Eur. Phys. J. B* **4**, 357 (1998).

²⁶J. Voit, *Rep. Prog. Phys.* **57**, 977 (1995).

²⁷M. Fabrizio, A. O. Gogolin, and S. Scheidl, *Phys. Rev. Lett.* **72**, 2235 (1995).

²⁸N. Nagaosa and A. Furusaki, *J. Phys. Soc. Jpn.* **63**, 413 (1995).

²⁹G. Cuniberti, M. Sassetti, and B. Kramer, *Europhys. Lett.* **37**, 421 (1997).

³⁰M. Sassetti and B. Kramer, *Phys. Rev. B* **55**, 9306 (1997).

³¹R. Egger and H. Grabert, *Phys. Rev. B* **55**, 9929 (1997).

³²H. Maurey and T. Giamarchi, *Europhys. Lett.* **38**, 681 (1997).

³³H. J. Schulz, *Phys. Rev. Lett.* **71**, 1864 (1993).

- ³⁴M. Abramowitz and I. A. Stegun, *Handbook of Mathematical Functions* (Dover, New York, 1965).
- ³⁵M. Sasseti and B. Kramer, Phys. Rev. B **54**, R5203 (1996).
- ³⁶M. Sasseti, F. Napoli, and U. Weiss, Phys. Rev. B **52**, 11 213 (1995).
- ³⁷A. Furusaki and K. A. Matveev, Phys. Rev. Lett. **75**, 709 (1995).
- ³⁸H. Yi and C. L. Kane, Phys. Rev. B **57**, 5579 (1998).
- ³⁹E. Lieb and D. Mattis, Phys. Rev. **125**, 164 (1962).
- ⁴⁰K. Jauregui, W. Häusler, D. Weinmann, and B. Kramer, Phys. Rev. B **53**, R1713 (1996).